RSC Advances

PAPER

View Article Online
View Journal | View Issue

Cite this: *RSC Adv.*, 2017, **7**, 8755

New insights into the activity of a biochar supported nanoscale zerovalent iron composite and nanoscale zero valent iron under anaerobic or aerobic conditions†

Xiangqi Peng,‡[a] Xiaocheng Liu,‡[a] Yaoyu Zhou,*[a] Bo Peng,[b] Lin Tang,*[b] Lin Luo,[a] Bangsong Yao,[c] Yaocheng Deng,[b] Jing Tang[b] and Guangming Zeng[b]

In this work, to gain insight into the mechanism of *p*-nitrophenol (PNP) removal using the reactivity of a biochar supported nanoscale zerovalent iron composite (nZVI/biochar) and nanoscale zero valent iron (nZVI) under anaerobic or aerobic conditions, batch experiments and models were conducted. The PNP removal rate in the more acidic solutions was higher, while it was significantly suppressed at higher pH, especially at pH 9.0. The peak value of the apparent rate constants suggests that the reactivity of nZVI/biochar could be much stronger than that of nZVI under the same aeration conditions. The modified Langmuir–Hinshelwood kinetic model could successfully describe the PNP removal process using nZVI/biochar or nZVI. The reaction constants obtained through a Langmuir–Hinshelwood mechanism under different aeration conditions followed the trend nZVI/biochar (N_2) > nZVI/biochar (air) > nZVI (N_2) > nZVI (air), indicating that nZVI/biochar under anaerobic conditions exhibits enhanced activity for the degradation of PNP. The nZVI/biochar under anaerobic conditions has the lowest Arrhenius activation energy of PNP degradation–adsorption, suggesting that the surface interaction of eliminating PNP has a low energy barrier. In addition, TOC removal under anaerobic conditions was negligible compared with that under the aerobic system and the total number of iron ions leaching at solution pH 3.0 in the nZVI/biochar or nZVI system under air aeration conditions was much higher than that under nitrogen aeration conditions. The profiles of the intermediates formed during the PNP degradation indicated that in the anaerobic environment, reduction was the predominant step in the removal process, while the degradation of PNP could be regarded as a combination of oxidation and reduction in an aerobic environment.

Received 24th November 2016
Accepted 12th January 2017

DOI: 10.1039/c6ra27256h

rsc.li/rsc-advances

1. Introduction

Iron is the fourth most plentiful element and the most abundant transition metal on earth.[1,2] Hence, various iron-containing materials have been investigated intensively and applied in the field of environmental protection. In the past two decades, zero valent iron (ZVI), especially, nanoscale zero valent iron (nZVI), has been widely studied for environmental remediation because of its greater specific surface area, possible nano-scale effects, environmental friendliness, and high reductive capacity (E_0 = −0.44 V), and the production of nontoxic iron oxides after the removal of pollutants.[2] nZVI is very versatile and it can act as a sorbent (*i.e.*, *via* the iron(hydr) oxide layer) for metals,[3] a reductant (*i.e.*, *via* Fe^0 and surface-bound Fe(II)) for environmental pollutants,[4] and a coagulant (*i.e.*, *via* dissolution of Fe(II) from the nZVI surface) for various anions in wastewater,[5] and meanwhile, it is also a heterogeneous Fenton regent for the advanced oxidation treatment of organic contaminants with an abundance of oxygen (*i.e.*, *via* Fe^0, Fe(II) and molecular oxygen to produce reactive oxygen species).[6] Therefore, nZVI has shown great potential for the remediation of wastewater and groundwater contaminated with a wide range of inorganic and organic pollutants.

Unfortunately, the agglomerate during the preparation process, the intrinsic characteristics of nZVI reacting with surrounded media, poor mobility and the formation of an iron oxide shell on nZVI are likely to reduce the reactivity the nanoparticles.[7–9] To solve these issues, nZVI-based materials, including porous material supported nZVI (*e.g.*, mesoporous silica,[10] resin[11] and nanoscale magnesium hydroxide[12]), carbon

[a]*College of Resources and Environment, Hunan Agricultural University, Changsha 410128, China. E-mail: zhouyy@hunau.edu.cn*

[b]*College of Environmental Science and Engineering, Hunan University, Changsha, 410082, China. E-mail: tanglin@hnu.edu.cn*

[c]*College of Engineering, Hunan Agricultural University, Changsha 410128, China*

† Electronic supplementary information (ESI) available. See DOI: 10.1039/c6ra27256h

‡ These authors contributed equally to this work.

material supported nZVI (*e.g.*, activated carbon,[13] carbon nanotubes,[14] graphene[15] and mesoporous carbons[4,16]), and inorganic clay mineral supported nZVI (*e.g.*, zeolite and montmorillonite,[17] diatomite,[18] and kaolinite[19]) have been synthesized to remove pollutants from environment. These supports can enhance the reactivity of nZVI. Thus, a competitive support should be cheap, safe and able to avoid negative influences caused by nZVI-based materials treatment.

Recently, biochar was introduced as a candidate to support nZVI by researchers for the following reasons: (i) biochar is cheap, non-toxic and easy to obtained, (ii) biochar can stabilize and disperse engineered nanoparticles, and thus enhance their mobility and stability, (iii) an increasing number of oxygen-containing functional groups on biochar's pore surface is highly useful for reducing metal leachability. Therefore, biochar supported nZVI has been used to treat some toxic and refractory pollutants (*e.g.*, metals, organochlorine compounds and nitro-aromatic compounds) in the industrial wastewater, and exhibited higher reactivity than nZVI.[2,20]

Besides, many factors were believed to affect the performance of nZVI towards pollutants removal. For examples, solution pH plays an important role in the negatively and positively charged surface species of nZVI-based materials, which may affect the removal of pollutants, and this factor also influence the production of reactive oxygen species (ROS) under aerobic conditions.[2,21] Some researchers reported that increasing solution pH could diminish the removal of polychlorinated biphenyls (PCBs),[22] Cr(VI),[23] 2,4-dichlorophenoxyacetic acid,[24] and phosphate,[25] but others found that the increasing solution pH could enhance the removal of cadmium[26] and antibiotics.[27] In addition, it has been reported that the dissolved oxygen (DO) could diminish the removal of some pollutants such as bromate[28] and trichloropropanone.[29] On the other hand, the presence of DO was believed to enhance the removal of chromate,[30] and dichloroacetic acid,[31] and other researcher found that the removal efficiency of trichloroacetic acid increased at first and then decreased with increasing DO concentrations.[31]

According to the above mentioned, it is important to better understand the effect of these factors such as solution pH and DO concentrations in order to gain insight into the suitability of nZVI application for removal of specific contaminants under certain environmental conditions. Although some researchers reported that the reactivity of nZVI towards heavy metals and organic compounds was high in anaerobic conditions, the reactivity of biochar supported nanoscale zerovalent iron composite (nZVI/biochar) towards *p*-nitrophenol (PNP) in aerobic or anaerobic conditions has not been systematically investigated. And its comparison to nZVI systems is an inevitable evaluation. Therefore, PNP, widely used as pharmaceuticals, dye and pesticides intermediates in agriculture or industry, selected as a model pollutant because of its reduced and oxidized abilities.

The objective of this study is to (i) evaluate the activation ability of nZVI/biochar for the removal of PNP in comparison to nZVI in aqueous solutions, (ii) elucidate mechanisms for removal of PNP using nZVI/biochar under anaerobic or aerobic conditions, and develop a kinetic model for the PNP removal using ZVI on the basis of the Langmuir–Hinshelwood model. This work provided us a simple low-cost method for the efficient elimination of environmental pollutants from wastewater.

2. Experimental

2.1. Materials, chemicals and preparation of nZVI/biochar

The used materials and chemicals are presented in Text S1 of ESI.† The preparation procedure of biochar and nZVI/biochar are described in Text S2 of ESI.†

2.2. Batch experiments

Preliminary experiments for the removal of PNP by biochar, nZVI/biochar and nZVI were described in Text S3 of ESI.† Besides, PNP degradation experiments were performed with two parameters as follows: (i) we carried out the batch experiments in which the solution pH was controlled to the specific pH (3.0, 5.0, 6.7 (natural pH), or 9.0) either by adding H_2SO_4 or NaOH. (ii) Air aeration (aerobic conditions) or purging with N_2 (anaerobic conditions). In addition, the purging rate was set up at 1 L min^{-1} referring to previous studies.[6] All analytical procedures for determination of the residual concentration of PNP, TOC, iron speciation, and main intermediates of *p*-aminophenol and *p*-benzoquinone were described in Text S4 of ESI† according to our previous work.[6]

2.3. Modeling

In this work, the pseudo-first-order was utilized to fit the experimental data because of the solid–liquid inter-phase reaction.[32] The kinetic rate equation is expressed in eqn (1).

$$\ln\frac{C_0}{C_t} = k_{obs}t \quad (1)$$

where C_0 and C_t (mg L^{-1}) are the initial concentration and the residual concentration of PNP at treatment time t (min), respectively, k_{obs} (min^{-1}) is the apparent rate constant, and k_{obs} is calculated by the method of linear regressions.

Generally, the heterogeneous reaction for the removal of organics encompasses with both degradation and adsorption that occurs simultaneously,[33,34] and can be described by the Langmuir–Hinshelwood mechanism.[34–36] The equation can be expressed as follows:

$$k_{obs} = \frac{k_c K_{LH}}{1 + K_{LH}C_0} \quad (2)$$

The linearized form of the Langmuir–Hinshelwood equation is:

$$\frac{1}{k_{obs}} = \frac{C_0}{k_c} + \frac{1}{k_c K_{LH}} \quad (3)$$

where the k_c is the intrinsic surface reaction rate constant (mg L^{-1} min^{-1}) and K_{LH} is the Langmuir–Hinshelwood adsorption equilibrium constant (L mg^{-1}). The values of k_c and K_{LH} can be calculated by plotting the ($1/k_{obs}$) against C_0.

The Arrhenius activation energy of degradation–adsorption step was determined using following eqn (4):

$$\ln k_{obs} = \ln A + \frac{(-E_a)}{RT} \quad (4)$$

where A is a constant, R is the gas constant (8.314 J mol^{-1} K^{-1}), T is the solution temperature and E_a is the activation energy.

3. Results and discussion

3.1. Characterization of nZVI/biochar

The morphologies of biochar and nZVI/biochar were observed using scanning electron microscope (SEM) (Fig. 1). The prepared nZVI was composed of fine spherical particles. The nZVI were homogeneously distributed across the entire biochar surface. In the X-ray diffraction (XRD) spectra (Fig. S1, ESI†), the broad XRD reflection peaks suggested the amorphous nature of biochar composite, and nZVI was believed to be present within the nZVI/biochar composite as indicated by diffraction peaks at 44.0° (corresponding to nZVI XRD patterns, JCPD 01-087-0721). The results indicated that the iron was deposited on the nZVI/biochar. According to the Debye–Scherrer formula $D = K\lambda/(B \cos \theta)$, where K is the Scherrer constant (0.89), k is the X-ray wavelength (0.15418 nm), b is the peak full width at half maximum and h is the Bragg diffraction angle. The calculated crystallite sizes were found to be 45.7 nm.

3.2. Effect of solution pH on removal of PNP under anaerobic and aerobic conditions

The reactivity of nZVI/biochar and nZVI for the removal of PNP solution (100 mg L^{-1}) at different pH values was investigated under aerobic and anaerobic conditions. As seen in Fig. S2,† the PNP degradation rates were fast in the first few minutes. In order to intuitively compare PNP degradation rates under different conditions, the pseudo-first-order was utilized to fit the experimental data, and the k_{obs} of different solution pH values under aerobic and anaerobic conditions were obtained. As seen in Fig. 2, it is observed that the logarithmic plots of residual concentration of PNP in aqueous solution *versus* the reaction time when the wastewater was treated by nZVI/biochar with various pH values under different aeration conditions. Besides, there was a good linear fitting in each batch experiment ($R^2 > 0.9391$), which indicates that all followed the pseudo-first-order kinetics model. The k_{obs} (>0.2409 min^{-1}) were obtained with various pH values under different aeration conditions (Table S1†). Fig. 2(A) show that the linear fitting of pseudo-first-order model (when the PNP aqueous solution was treated by nZVI/biochar system with pH values from 3.0 to 9.0 under anaerobic conditions). As presented in Table S1,† the k_{obs} decreased from 0.5283 to 0.3360 min^{-1} with increasing pH. Additionally, the k_{obs} (from 0.4971 to 0.2409 min^{-1}) of nZVI/biochar systems with pH values from 3.0 to 9.0 under aerobic conditions were below those obtained under the anaerobic conditions. This phenomenon could be explained in the following three aspects, (a) under anaerobic conditions, the nitrogen aeration could eliminate the dissolved oxygen in PNP aqueous solution and maintain the anaerobic conditions, and thus, enhanced the reduction reactivity of Fe^0.[4,6] (b) Previous work indicated that PNP was relatively easy to be reduced into *p*-aminophenol, but on the contrary, PNP with the benzene ring was very hard to be opened by oxidation.[6,37,38] (c) The nitrogen was favor to the fluidization of Fe^0 particles in the reaction process,[37] and thus could enhance the corrosion products, radicals, mass transfer rate of PNP and intermediates between the surface of Fe^0 particles and aqueous solution. It has been reported that the degradation efficiency of pollutant could enhance the acceleration of mass transfer rate.[39,40]

As for nZVI, no matter under anaerobic or aerobic conditions, it was clear that the k_{obs} obtained in nZVI/biochar systems were obviously higher than those obtained in nZVI systems at pH from 3.0 to 9.0. Especially, under the anaerobic and aerobic conditions, the k_{obs} (0.3360 and 0.2409 min^{-1}) obtained in nZVI/biochar systems were approximate 15 and 20 times higher than those (0.0224 and 0.0115 min^{-1}) obtained in nZVI systems at pH 9.0, respectively. The results strongly revealed that nZVI/biochar can provide excellent performance for the removal of PNP in comparison to nZVI. The relative low removal efficiency of non-supported nZVI can be attributed to the aggregation of the iron nanoparticles. Yan *et al.* also found that the non-supported nZVI would decrease the removal efficiency of organic compound by Fe^0.[20] Moreover, no matter under which conditions, it is observed that the obtained k_{obs} diminished with the increased pH from 3.0 to 9.0. The results could be explained in three main aspects. (a) Since the corrosion rate of Fe^0 was very low under higher pH, $^{\cdot}H$ was hard to be generated to reduce the pollutants. (b) The corrosion reaction of nZVI was

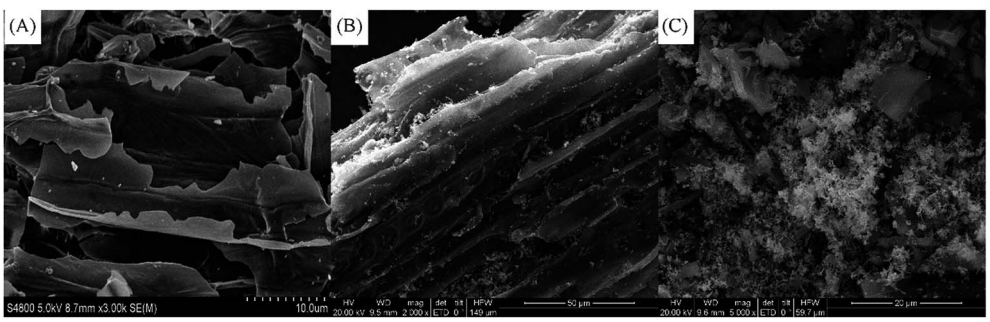

Fig. 1 SEM images of biochar (A), nZVI/biochar of (B, image scale of 50 μm), nZVI/biochar (C, image scale of 20 μm).

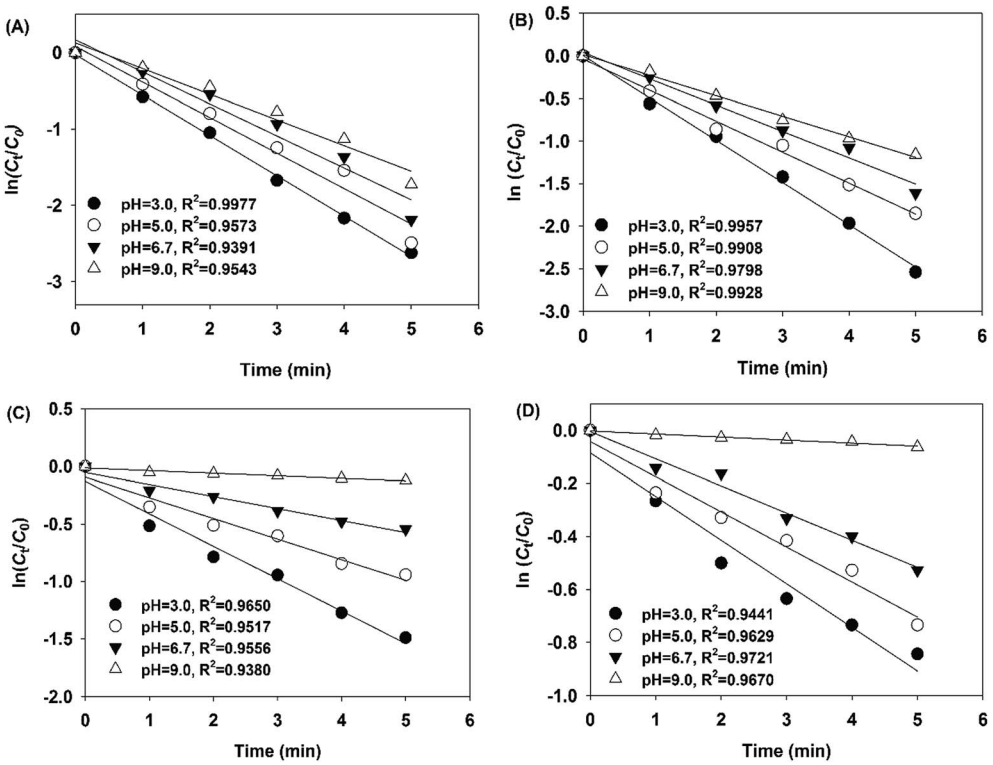

Fig. 2 Linear fitting using pseudo-first-order model. Reaction conditions: PNP degradation for nZVI/biochar or nZVI systems with various pH values under different aeration conditions with initial PNP concentration of 100 mg L^{-1}, temperature at 25 ± 2 °C and contact time of 180 min. nZVI/biochar (A) and nZVI (B) purging with N_2, nZVI/biochar (C) and nZVI (D) with air aeration.

hard to be performed efficiently in the absence of H^+, which inhibited the release of electrons from nZVI, and thus, O_2 could not obtain enough electrons to be reduced into H_2O_2. (c) Both H^+ and O_2 were very important in the generation of H_2O_2 in nZVI system,[37] and in the absence of H^+, the H_2O_2 was hard to be formed in nZVI system, even if enough dissolved oxygen (DO) was added. Therefore, the low k_{obs} of nZVI system was obtained under higher pH.

3.3. Kinetic study

In this work, the heterogeneous reaction for the removal of PNP was described by the Langmuir–Hinshelwood model. In addition, the Arrhenius model was used to calculate the activation energy of degradation–adsorption PNP. Fig. S3 and S4† illustrate the dependence of PNP degradation by nZVI/biochar or nZVI systems on the initial concentration of PNP ranging from 100 to 600 mg L^{-1} under anaerobic or aerobic conditions. The profile of normalised concentrations with time was described the degradation of PNP according to the pseudo-first-order kinetics. The slope of the straight line for a plot of $\ln(C_t/C_0)$ *versus* t determines the k_{obs} value (summarized in Table S2†). The results in this work showed that the k_{obs} values decreased as the initial concentration increased.

As seen in Fig. 3, the Langmuir–Hinshelwood model is used to simulate the kinetics of PNP degradation by nZVI/biochar or nZVI. It can be seen that the correlation coefficients are very close to 1, which indicates that the kinetics of PNP by nZVI/biochar or nZVI can be described by the Langmuir–Hinshelwood model very well. Zhang *et al.* found the kinetics of degradation of atrazine by nZVI supported on organobentonite or nZVI followed well with the Langmuir–Hinshelwood equation. Zhang and co-worker found that both the adsorption and catalysis coexisted in the hydrophobic phase, and the reaction mainly occurred in the interlayers.[41] In this study, the reaction rate constant ($k_{c\text{-}1}$) for the nZVI/biochar treatment is larger than that for the nZVI treatment, indicating that the reaction rate is positively related to the adsorption on nZVI/biochar.

The kinetic and thermodynamic parameters of the catalytic reduction of PNP are important as far as industrial wastewater treatment concerned. The reaction rate constants (k) are calculated according to pseudo-first-order kinetic model. The plots of ln C/C_0 *versus* t at 288, 293 and 298 K, and the values of reaction rate constant and correlation coefficients are listed in Fig. S5† and the inset figure, respectively. The Arrhenius activation energy of degradation–adsorption step was determined using eqn (4). The activation energy of nZVI/biochar or nZVI systems on the removal of PNP under anaerobic and aerobic conditions were also summarized in Fig. S6† inset. It is clear that nZVI/biochar under anaerobic condition has the lowest activation energy, indicates the surface interaction of eliminating PNP has low energy barrier.

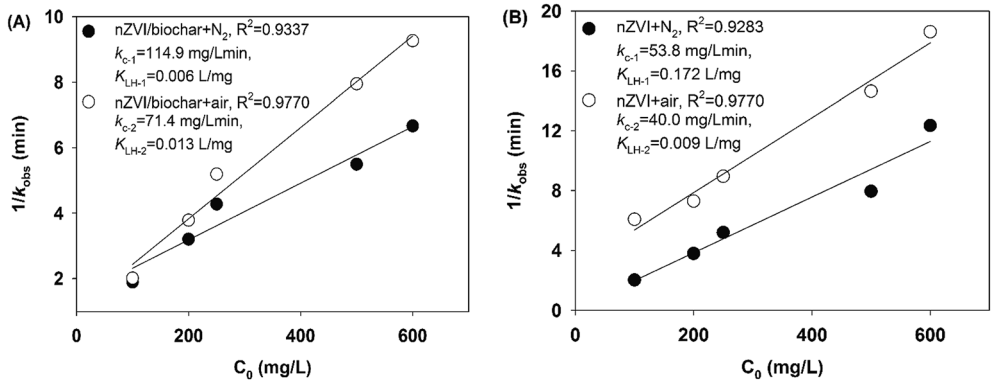

Fig. 3 Relationship between the $1/k_{obs}$ and concentration of PNP using Langmuir–Hinshelwood model, nZVI/biochar (A) and nZVI (B) systems at pH 3.0 under different aeration conditions with initial PNP concentration from 100 mg L^{-1} to 600 mg L^{-1}, temperature at 25 ± 2 °C.

3.4. TOC removal, total iron ions leaching under the anaerobic and aerobic conditions

Fig. 4 shows the plots of TOC/TOC_0 after 180 min treatment under anaerobic and aerobic conditions at pH 3.0. The TOC removal of PNP under aerobic conditions was more obvious than that in anaerobic conditions no matter in nZVI/biochar or nZVI systems. The phenomenon could be explained by the theory that the benzene ring of PNP could not be opened under anaerobic conditions, while in aerobic conditions the cleavage of benzene ring of PNP happened and the generated ·OH radicals occurred in the removal of TOC.[6,37] It is clear from the results for TOC removal under anaerobic and aerobic conditions was mainly attributed to reductive degradation rather than oxidative degradation.

In addition, Fig. 4 shows the plots of the leaching of total iron ions at pH 3.0 after 50 min treatment under anaerobic and aerobic conditions. It can be observed that nZVI/biochar or nZVI in the anaerobic system the leaching of total iron ions at pH 3.0 was significantly below the value in the aerobic system. Despite the lower iron leaching rate, the electrons emitted by nZVI/biochar or nZVI dissolution were adequate for reductive degradation of PNP and the intermediate, due to the iron oxide layer or passive layer was not formed at pH 3.0. Tang *et al.* also found the similar results that in the anaerobic system the leaching of total iron ions in acidic conditions significantly lowered, and the rate of pollutant removal in the anaerobic system was comparable to that in the aerobic system.[6] Moreover, iron ions could cause a secondary pollution in the environment. One can see from Fig. 4 that the concentration of iron ions in the solution was high in the removal of PNP by nZVI. However, for the nZVI/biochar treatment, much fewer iron ions were detected. The reason may be that the interactions between iron ions and biochar prevented the iron ions from being released into the solution. A similar result has been observed by using bentonite, alginate bead and pristine pinewood derived biochars as a carrier of nZVI.[2,41,42]

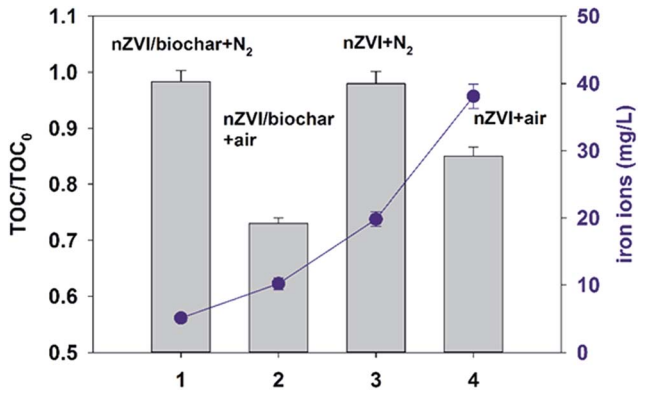

Fig. 4 TOC removal and total iron ions leaching in the removal of PNP in nZVI/biochar or nZVI systems at pH 3.0 treatment purging with N_2 or air, with initial PNP concentration of 100 mg L^{-1} and temperature at 25 ± 2 °C, errors bars indicating standard deviations.

3.5. Proposed reaction pathway for degradation of PNP with nZVI/biochar

As described previously, reduction and oxidation could degrade PNP, and the degradation of PNP in nZVI system might occur through multiple pathways, *p*-aminophenol, *p*-benzoquinone and hydroquinone have been identified as the main intermediates in PNP degradation processes.[6,36,38,43] Under anaerobic conditions, the reduction of nitro-group ($-NO_2$) in PNP into amino-group ($-NH_2$) is a dominant reaction in the reductive degradation of PNP in nZVI system. On the other hand, *p*-benzoquinone and hydroquinone have been identified as primary intermediate formed by the reaction of PNP under aerobic conditions with ·OH radicals. Therefore, in this work, we detected the concentrations of main intermediates of *p*-aminophenol (standing for reduction products) and *p*-benzoquinone (standing for oxidation products), and the result was presented in Fig. 5. It is observed that the *p*-aminophenol concentration rapidly increased during the first 10 min, and then rapidly decayed. In addition, the *p*-benzoquinone concentration increased slightly. The phenomena demonstrated that the degradation process of PNP under aerobic conditions could be regarded as an oxidation combined with a reduction. Similar results were found in our previous work using sulfidated nanoscale zerovalent iron for the removal of

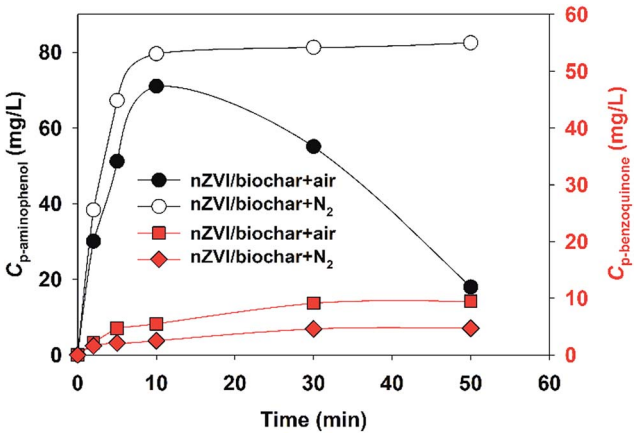

Fig. 5 Concentrations of *p*-aminophenol and *p*-benzoquinone under purging with N_2 or air treatment by nZVI/biochar with initial PNP concentration of 100 mg L^{-1}, temperature at 25 ± 2 °C and contact time of 50 min.

PNP.[6] Nakatsuji *et al.* using zero-valent iron for the degradation of PNP also found similar results.[43] However, the main product was *p*-aminophenol under anaerobic conditions, indicates that the main degradation process of PNP was regarded as a reduction under anaerobic conditions. The proposed reaction pathway for degradation of PNP with nZVI/biochar was presented in Fig. S7.†

4. Conclusions

In this study, it was demonstrated that the effect of aeration conditions on the removal of PNP by nZVI/biochar or nZVI system. The results suggest that the reactivity of nZVI/biochar could be much stronger than that of nZVI under the same aeration condition. The peak value of PNP apparent rate constants, calculated by the pseudo first-order kinetics equation, appeared at pH 3.0 in the pH range of 3.9–9.0 in the nZVI/biochar or nZVI system under anaerobic conditions. Particularly, a kinetic model for the PNP removal by using nZVI/biochar or nZVI was developed on the basis of the Langmuir–Hinshelwood model. The data of PNP removal fitted well with the Langmuir–Hinshelwood model. The reaction constant of nZVI/biochar was much higher than that of nZVI under the same aeration conditions, especially, the reaction constant of nZVI/biochar under anaerobic conditions. It demonstrated that the reaction rate is positively on nZVI/biochar. TOC removal efficiencies and total iron ions leaching at pH 3.0 obtained by nZVI/biochar or nZVI system under air aeration conditions were much higher than those obtained under nitrogen aeration conditions. The dominant reaction pathway under the anaerobic conditions was nitro-group of PNP reduction to the amino group. Under the air aeration conditions, the degradation process of PNP by nZVI/biochar could be regarded as an oxidation combined with a reduction. Taken together, considering the cost-effectiveness and environmental safety, nZVI/biochar may be a more suitable alternative to nZVI for enhanced reactivity for the degradation of nitroaromatic compounds.

Acknowledgements

The study was financially supported by Projects Projects 51222805, 51579096, 51521006, 31272248 and 51508175 supported by National Natural Science Foundation of China, the National Program for Support of Top-Notch Young Professionals of China (2012), and the Program for New Century Excellent Talents in University from the Ministry of Education of China (NCET-11-0129). Project of Science and Technology of Hunan Province (2015WK3016).

References

1 Y. Sun, J. Li, T. Huang and X. Guan, *Water Res.*, 2016, **100**, 277–295.
2 S. Wang, B. Gao, Y. Li, A. E. Creamer and H. Feng, *J. Hazard. Mater.*, 2017, **322**, 172–181.
3 X. Guo, Y. Zhe, H. Dong, X. Guan, Q. Ren, X. Lv and J. Xin, *Water Res.*, 2015, **88**, 671–680.
4 Y. Zhou, L. Tang, G. Yang, G. Zeng, Y. Deng, B. Huang, Y. Cai, J. Tang, J. Wang and Y. Wu, *Catal. Sci. Technol.*, 2015, **6**, 1930–1939.
5 X. Li, L. Ai and J. Jing, *Chem. Eng. J.*, 2016, **288**, 789–797.
6 J. Tang, L. Tang, H. Feng, G. Zeng, H. Dong, Z. Chang, B. Huang, Y. Deng, J. Wang and Y. Zhou, *J. Hazard. Mater.*, 2016, **320**, 581–590.
7 M. Stefaniuk, P. Oleszczuk and S. O. Yong, *Chem. Eng. J.*, 2016, **287**, 618–632.
8 E. Lefevre, N. Bossa, M. R. Wiesner and C. K. Gunsch, *Sci. Total Environ.*, 2016, **565**, 889–901.
9 D. L. Huang, G. M. Zeng, C. L. Feng, S. Hu, X. Y. Jiang, L. Tang, F. F. Su, Y. Zhang, W. Zeng and H. L. Liu, *Environ. Sci. Technol.*, 2008, **42**, 4946–4951.
10 E. Petala, K. Dimos, A. Douvalis, T. Bakas, J. Tucek, R. Zbořil and M. A. Karakassides, *J. Hazard. Mater.*, 2013, **261**, 295–306.
11 Q. Du, S. Zhang, B. Pan, L. Lv, W. Zhang and Q. Zhang, *Water Res.*, 2013, **47**, 6064–6074.
12 M. Liu, Y. Wang, L. Chen, Y. Zhang and Z. Lin, *ACS Appl. Mater. Interfaces*, 2015, **7**, 7961–7969.
13 W. F. Chen, L. Pan, L. F. Chen, Q. Wang and C. C. Yan, *RSC Adv.*, 2014, **4**, 46689–46696.
14 G. Sheng, A. Alsaedi, W. Shammakh, S. Monaquel, J. Sheng, X. Wang, H. Li and Y. Huang, *Carbon*, 2015, **99**, 123–130.
15 H. Jabeen, K. C. Kemp and V. Chandra, *J. Environ. Manage.*, 2013, **130C**, 429–435.
16 Y. Deng, L. Tang, G. Zeng, J. Wang, Y. Zhou, J. Wang, J. Tang, Y. Liu, B. Peng and F. Chen, *J. Mol. Catal. A: Chem.*, 2016, **421**, 209–221.
17 N. Arancibia-Miranda, S. E. Baltazar, A. García, D. Muñoz-Lira, P. Sepúlveda, M. A. Rubio and D. Altbir, *J. Hazard. Mater.*, 2015, **301**, 371–380.
18 L. Ma, H. He, R. Zhu, J. Zhu, I. D. R. Mackinnon and Y. Xi, *Catal. Sci. Technol.*, 2016, **6**, 6066–6075.
19 Z. Chen, T. Wang, X. Jin, Z. Chen, M. Megharaj and R. Naidu, *J. Colloid Interface Sci.*, 2013, **398**, 59–66.

20 J. Yan, H. Lu, W. Gao, X. Song and M. Chen, *Bioresour. Technol.*, 2014, **175**, 269–274.
21 H. Su, Z. Fang, P. E. Tsang, L. Zheng, W. Cheng, J. Fang and D. Zhao, *J. Hazard. Mater.*, 2016, **318**, 533–540.
22 Y. Wang, D. Zhou, Y. Wang, L. Wang and C. Long, *Environ. Sci. Pollut. Res.*, 2012, **19**, 448–457.
23 L. Wu, L. Liao, G. Lv and F. Qin, *J. Contam. Hydrol.*, 2015, **179**, 1–9.
24 A. C. D. Velosa and R. F. P. Nogueira, *J. Environ. Manage.*, 2013, **121**, 72–79.
25 Z. Wen, Y. Zhang and C. Dai, *Colloids Surf., A*, 2014, **457**, 433–440.
26 Y. Su, A. S. Adeleye, Y. Huang, X. Sun, C. Dai, X. Zhou, Y. Zhang and A. A. Keller, *Water Res.*, 2014, **63**, 102–111.
27 W. Liu, J. Ma, C. Shen, Y. Wen and W. Liu, *Water Res.*, 2015, **90**, 24–33.
28 L. Xie and C. Shang, *Chemosphere*, 2007, **66**, 1652–1659.
29 J. Y. Lee, R. M. Hozalski and W. A. Arnold, *Chemosphere*, 2007, **66**, 2127–2135.
30 P. Feng, X. Guan, Y. Sun, W. Choi, H. Qin, J. Wang, J. Qiao and L. Li, *J. Environ. Sci.*, 2015, **31**, 175–183.
31 S. Tang, X. M. Wang, Y. Q. Mao, Y. Zhao, H. W. Yang and Y. F. Xie, *Water Res.*, 2015, **73C**, 342–352.
32 X. Luo, S. Zhang and X. Lin, *J. Hazard. Mater.*, 2013, **260C**, 112–121.
33 L. Lin, H. Wang and P. Xu, *Chem. Eng. J.*, 2017, **310**, 389–398.
34 X. Wang, Y. Qin, L. Zhu and H. Tang, *Environ. Sci. Technol.*, 2015, **49**, 6855–6864.
35 A. Idris, N. Hassan, R. Rashid and A. F. Ngomsik, *J. Hazard. Mater.*, 2009, **44**, 1683–1688.
36 P. Guo, L. Tang, J. Tang, G. Zeng, B. Huang, H. Dong, Y. Zhang, Y. Zhou, Y. Deng and L. Ma, *J. Colloid Interface Sci.*, 2016, **469**, 78–85.
37 Z. Xiong, L. Bo, Y. Ping, Y. Zhou, J. Wang and S. Fang, *J. Hazard. Mater.*, 2015, **297**, 261–268.
38 L. Tang, J. Tang, G. Zeng, G. Yang, X. Xie, Y. Zhou, Y. Pang, Y. Fang, J. Wang and W. Xiong, *Appl. Surf. Sci.*, 2015, **333**, 220–228.
39 B. Lai, Z. Chen, Y. Zhou, P. Yang, J. Wang and Z. Chen, *J. Hazard. Mater.*, 2013, **250–251**, 220–228.
40 H. M. Hung, F. H. L. And and M. R. Hoffmann, *Environ. Sci. Technol.*, 1998, **32**, 3011–3016.
41 Y. Zhang, Y. Li and X. Zheng, *Sci. Total Environ.*, 2011, **409**, 625–630.
42 H. Kim, H. J. Hong, J. Jung, S. H. Kim and J. W. Yang, *J. Hazard. Mater.*, 2010, **176**, 1038–1043.
43 Y. Nakatsuji, Z. Salehi and Y. Kawase, *J. Environ. Manage.*, 2015, **152**, 183–191.